Volcanic shutdown of the Panama Canal area following breakup of the Farallon plate

David M. Buchs[a,b,*], Henry Coombs[a], Derek Irving[c], JianWang[a], Anthony Koppers[d], Roberto Miranda[c], Maurylis Coronado[c], Arkin Tapia[e], Samuel Pitchford[a]

[a] School of Earth and Ocean Sciences, Cardiff University, UK
[b] Smithsonian Tropical Research Institute, Panama
[c] Engineering Division, Panama Canal Authority, Panama
[d] College of Earth, Ocean and Atmospheric Sciences, Oregon State University, USA
[e] Instituto de Geociencias, University of Panama, Panama
[*] Corresponding author E-mail address: buchsd@cardiff.ac.uk (D.M. Buchs).

Abstract

The Panama Canal area is a significant part of the Panama Isthmus, where prominent volcanic fronts of eastern Central America are interrupted by a topographic low of unclear tectonic and magmatic origin. Determining why no prominent volcanic system occurs along the Canal is essential to understand the formation of the Isthmus in an area believed to have hosted one of the last inter-American straits between the Atlantic and Pacific Oceans. We provide here new geochronological and geochemical constraints from volcanic units of the Panama Canal that belong to the recently-identified Central Panama Volcanic Field. Whole rock and mineralogical geochemical compositions document a secular magmatic change from ca. 25 to 16Ma, with a progressive change from calcalkaline to tholeiitic and possibly alkaline/transitional geochemical affinities. The age of the youngest volcanic unit of the Canal is similar to that of the youngest documented arc volcanism in eastern Panama ca. 18 Ma. We propose based on these observations and consistency with regional geological constraints that the Canal volcanism represents a unique example of magmatic cessation along a volcanic arc. This cessation occurred shortly after the breakup of the Farallon plate ca. 23 Ma, suggesting a causal link between volcanic shutdown and transition from orthogonal to oblique subduction along Central and Eastern Panama. We suggest that this tectonic event suppressed hydrous melting in the subduction zone and led to regional magmatic waning in Central and Eastern Panama ca. 16Ma. The pre-existence of a transisthmian fault system in Central Panama probably facilitated extraction of the last supra-subduction melts during volcanic shutdown. Our results suggest that the end of volcanism, combined with transisthmian faulting, impeded the development of high topography in the Panama Canal area. Without this unusual tectono-magmatic evolution, the occurrence of a late inter-oceanic strait in Central Panama and the construction of the Panama Canal would not have been possible.

1. Introduction

The Panama Canal area corresponds to a distinctive topographic low approximately 50 km wide in Central Panama, which separates Palaeogene and Neogene volcanic fronts that form a prominent mountainous topography along the Panama Isthmus (Fig. 1). Because of this low topography and local preservation of Neogene marine sedimentary deposits, the Panama Canal area is generally believed to have hosted an interoceanic strait between the Atlantic and Pacific Oceans shortly before final emergence of the Isthmus in the Neogene (Collins et al., 1996; Kirby et al., 2008; MacFadden et al., 2017; Montes et al., 2015). The closure of inter-oceanic strait(s) during the formation of the Isthmus is a significant geological process that has been linked to a large range of global palaeo-oceanographic changes and inter-American biotic events (e.g., Haug and Tiedemann, 1998; Marshall et al., 1982; O'Dea et al., 2016). However, there are still very limited direct geological constraints on the evolution of the palaeogeographic evolution of the Isthmus, with final emergence generally constrained based on indirect palaeo-oceanographic and tectonic proxies (Bacon et al., 2015; Keigwin, 1982; Montes et al., 2015; O'Dea et al., 2016). To better understand the mode and timing of formation of the Isthmus, it is critical to provide new constraints on the volcanic and tectono-magmatic evolution of Panama.

Post-print version of Buchs et al. (2019)
https://doi.org/10.1016/j.lithos.2019.02.016

Final emergence of the Panama Isthmus is generally interpreted to be related to tectonic uplift due to collision of the Panama volcanic arc with South America (Coates et al., 2004; Farris et al., 2011; Montes et al., 2012a; Montes et al., 2015). However, magmatism and volcanic construction could also have played a significant role in the emergence of volcanic cordilleras (Buchs et al., 2019; Wörner et al., 2005), but the effects and extent of these processes remain poorly investigated in most of the Isthmus. Because of the peculiar topography of Central Panama and its role in the final emergence of the Isthmus, it is significant to characterise the origin and evolution of magmatism in the Canal area. We present here new geochronological and geochemical data from volcanic sequences recently exposed during the expansion of the Canal and show that they preserve a unique record of volcanic cessation, which played an important role in the establishment of the unique topography of Central Panama.

2. Geological background

Central Panama is characterised by an abrupt change in regional topography that correlates to a complex NW-SE striking fault system thought to extend from the Panama Canal area to the Pearl Islands and Sapo Range in eastern Panama (Barat et al., 2014; Mann and Kolarsky, 1995) (Fig. 1). Low topography of Central Panama also correlates to an age discontinuity in taller volcanic cordilleras, with an extinct Palaeogene volcanic front to the east (Lissinna, 2005; Maury et al., 1995; Montes et al., 2012b; Wegner et al., 2011), and an active Neogene volcanic front to the west (Defant et al., 1992; Lissinna, 2005; Wegner et al., 2011) (Figs. 1–2). The atypical curvilinear shape of the Panama Isthmus is thought to have formed due to collision of Panama with South America, which caused oroclinal bending of volcanic fronts combined with left-lateral offset along the central Panamanian fault zone since ca. 40–32 Ma (Barat et al., 2014; Mann and Corrigan, 1990; Montes et al., 2012b; Silver et al., 1990). Oroclinal deformation was coeval with migration of volcanic fronts in the Eocene, including: (i) northward relocation of the locus of volcanism from the Azuero-Sona Arc to the Central Cordillera in western Panama (Buchs et al., 2010; Lissinna, 2005; Wegner et al., 2011); and (ii), southward relocation of the locus of volcanism from the Chagres-Bayano Arc and San Blas Cordillera to the Majé Range and possibly other parts of eastern Panama (Lissinna, 2005; Whattam et al., 2012). Overall, existing regional data indicate that the Panama Canal area corresponds to a complex zone of structural transition between at least two dissected volcanic fronts. Significantly, although central and eastern Panama are volcanically inactive today (in the so-called "Darien Gap"), the timing and cause(s) of volcanic cessation in this region remain undocumented.

The study of the volcanic and magmatic evolution of Central Panama between the Oligocene and Miocene has recently focused on volcanogenic units of the Canal area (Farris et al., 2011, 2017; Rooney et al., 2011) that postdate an uplifted Maastrichtian to Eocene volcanic basement which is part of the nearby Chagres-Bayano Arc (Montes et al., 2012b; Wegner et al., 2011; Wörner et al., 2005) (Fig. 1). Rooney et al. (2011) document amphibole-bearing andesites (Cerro Patacon unit), which record formation of water-saturated magmas in the Canal area during the Oligocene. Farris et al. (2011, 2017) recognised Miocene tholeiitic series along the Gaillard Cut of the Panama Canal, which they propose reflect an atypical phase of anhydrous magmatism during a rifting event ca. 23 Ma. This possible rifting has been interpreted to be associated with internal deformation of Central Panama during collision of the Panama volcanic arc with South America. We present here a new regional synthesis and novel data from the Panama Canal, which support an alternate model of magmatic evolution of Central Panama related to regional volcanic shutdown, without causal link to collision of Panama with South America. Specifically, three new datasets are provided herein, that are key to unravelling the tectono-magmatic evolution of the Canal area: (i) Ar-Ar geochronological and whole rock geochemical results from the youngest in situ igneous rocks of the area (Pedro Miguel Formation); (ii) an Ar-Ar age for a dyke of an earlier dacite (Las Cascadas magmatic group) in the southern Gatun Lake; and (iii) geochemical analysis of magmatic pyroxenes from all magmatic groups of the Panama Canal and a sample of sandstone from pre-Oligocene volcanic arc sequences in Central Panama (Chagres-Bayano Arc of Wegner et al., 2011).

3. Methods

3.1. Field work and sampling

Field work and sampling were conducted during 6 field campaigns between 2015 and 2018 in (i) the Gaillard Cut and Pacific Locks area of the Panama Canal (286 localities), and (ii) nearby forested and urbanised areas in Central Panama (452 localities) (Buchs et al., 2019). Our survey was designed to provide new, systematic constraints on volcanic processes recorded in new exposures of the Gaillard Cut and Pacific locks area created during widening of the Canal since 2008, as well as their possible lateral equivalents along nearby rivers and roadcuts in Central Panama. Our study partly built upon previous results by Farris et al. (2017) and was carried out in collaboration with the Panama Canal Authority that has done detailed lithological and structural mapping of the Gaillard Cut and Pacific locks area during recent expansion of the Canal. Our study additionally benefited from access to a large collection of cores collected during the expansion. Field observations were complemented by microscope petrographic observations of 101 thin sections of volcanic and volcaniclastic rocks from the Gaillard Cut and Pacific locks area. Petrographic characteristics of igneous rocks collected along the Panama Canal are given in Table S1. The location of new analyses of igneous rocks that are considered in this study is illustrated in Supplementary Fig. S1 (coordinates in Table S2 and Buchs et al., 2019). A revised lithostratigraphy and volcanic constraints on the newly-introduced "Central Panama Volcanic Field" are detailed in Buchs et al. (2019).

3.2. Ar-Ar dating and age compilation

Eight new 40Ar/39Ar ages were obtained by incremental heating on feldspar and matrix of 7 samples of basalt to dacite/microgranodiorite from the southern Gatun Lake to Pacific entrance of the Panama Canal. The ages were obtained by incremental heating methods using the ARGUS-VI mass spectrometer at Oregon State University (OSU) Argon Geochronology Laboratory. Samples were irradiated for 6 h (14-OSU- 02) in the TRIGA CLICIT nuclear reactor at OSU, along with the FCT sanidine (28.201±0.023 Ma, 1σ) flux monitor (Kuiper et al., 2008). Individual J-values for each sample were calculated by parabolic extrapolation of the measured flux gradient against irradiation height and typically give 0.1–0.2% uncertainties (1σ). The 40Ar/39Ar incremental heating age determinations were performed on a multi-collector ARGUS-VI mass spectrometer at OSU that has 5 Faraday collectors (all fitted with 1012 Ohm resistors) and 1 ion-counting CuBe electron multiplier (located in a position next to the lowest mass Faraday collector). This allows us to measure simultaneously all argon isotopes, with mass 36 on the multiplier and masses 37 through 40 on the four adjacent Faradays. This configuration provides the advantages of running in a full multi-collector mode while measuring the lowest peak (on mass 36) on the highly sensitive electron multiplier (which has an extremely low dark-noise and a very high peak/noise ratio). Irradiated samples were loaded into Cu-planchettes in an ultra-high vacuum sample chamber and incrementally heated by scanning a defocused 25W CO2 laser beam in preset patterns across the sample, in order to release the argon evenly. After heating, reactive gases were cleaned up using an SAES Zr-Al ST101 getter operated at 400 °C for several minutes and two SAES Fe-V-Zr ST172 getters operated at 200 °C and room temperature, respectively. All ages were calculated using the corrected decay constant (Steiger and Jäger, 1977) of 5.530 ± 0.097 × 10–10 1/yr (2σ) as reported by Min et al. (2000). Incremental heating plateau ages and isochron ages were calculated as weighted means with 1/σ2 as weighting factor and as YORK2 least-square fits with correlated errors using the ArArCALC v2.7.2 software (Koppers, 2002) available from the http://earthref.org/ArArCALC/ website. Results are presented in Table 1, Supplementary File 1 and Fig. 2. Ar-Ar ages presented in this manuscript and Buchs et al. (2019) have consistent plateau and isochron ages that are also remarkably consistent with stratigraphic controls along the Gaillard Cut. Fig. 2 presents a synthesis of other Ar-Ar and U-Pb geochronological constraints from igneous rocks of the Canal area (Bloch et al., 2016; Buchs et al., 2019; MacFadden et al., 2014; Montes et al., 2012a; Rooney et al., 2011) and volcanic arcs of Panama (Baker et al., 2016; Lissinna, 2005; Montes et al., 2012b; Wegner et al., 2011;Whattamet al., 2012), which were included in our interpretations and model.

3.3. Whole rock geochemistry and data compilation

Major and trace elements of 28 samples of basalt/gabbro to andesite/ diorite from the Pedro Miguel Formation were analysed by ICP-OES and ICP-MS at the School of Earth and Ocean Sciences at Cardiff University, using the methods described in Buchs et al. (2019). Analytical results of the samples and standards are given in Table S2. Interpretation of the new data was carried out in comparison to a compilation of previous geochemical results from the Panama Canal area (Buchs et al., 2019; Farris et al., 2017; Rooney et al., 2011), the Chagres-Bayano Arc (Wegner et al., 2011) and the recent arc of Panama as depicted in Fig. 1 (Baker et al., 2016; Wegner et al., 2011; Whattam et al., 2012). Comparison with pre-Oligocene volcanic arc sequences was restricted to the Chagres-Bayano Arc of Wegner et al. (2011) due to its proximity to the Canal area, and to minimise bias due to possible along-strike chemical variability and limited geochronological control in the older segments of the arc (Figs. 1–2). Trace elements analysed by XRF and INAA in Farris et al. (2011, 2017) were not used here due to analytical discrepancies with previous and new results (in particular Nb). However, ICP-MS results from Farris et al. (2017) were used when available. For the interpretation of elements known to be mobile during weathering and alteration (e.g., K, Na and Ba), we did not consider samples with a total of oxides <96 wt% (assuming this reflects high abundance of secondary hydrous minerals and/or carbonate). Major element contents were recalculated on an anhydrous basis or to a total of 100 wt% in the absence of loss on ignition (LOI). As discussed below this conservative approach led to significant differences of observation with some of the previous studies in the Canal area.

3.4. Clinopyroxene geochemistry

Chemical microanalyses of clinopyroxenes from 17 samples (555 analyses) were carried out using a Zeiss Sigma HD Analytical Scanning Electron Microscope (SEM) at Cardiff University equipped with dual 150mm2 active area EDS detectors and Oxford Instruments Aztec software. A beam energy of 20 kV was used with a nominal beam current of ~1 nA. The analyses were fully standardised with elements calibrated using mineral standards from Astimex Standards Ltd. and Smithsonian Microbeam Standards. Accuracy and precision were measured using repeated spot analysis of chrome diopside and augite. Beam drift was measured every 15min using Co as a reference standard. Samples and standards results are given in Table S3. The analysis of standards shows that elements in pyroxenes have an average relative error generally <10%, specifically of ~1% for Ca, 2–8% for Na, 1–15% for Ti, and 4–18% for Cr (close to its detection limit of ~0.10 wt%). Thus, SEM analytical error is significantly lower than natural variability and geochemical trends documented in this study. Individual plotting of samples in Mg#-Ti and discrimination diagrams of Leterrier et al. (1982) are given in Supplementary File 2 (see text for comments).

4. Results

4.1. Geochemical groups

The magmatic evolution of the Panama Canal area can be characterised using 4 main geochemical groups that show excellent internal petrological consistency and correlate to units defined by clear lithostratigraphic and chronostratigraphic criteria (Fig. 2B):

1) The Cerro Patacon group corresponds to an andesitic series sampled and dated ca. 25Ma in the Cerro Patacon area, approximately 6 km east to Panama Canal (Rooney et al., 2011).
2) The Bas Obispo group corresponds to the formation of the same name in the northern Gaillard Cut. Originally interpreted as pyroclastic deposits (Farris et al., 2017; Montes et al., 2012a), new observations show that this formation consists of fluvial deposits with rounded clasts of basalt to basaltic andesite dated ca. 25–24 Ma (Buchs et al., 2019). These ages indicate that emplacement of the Bas Obispo basalts was coeval to that of the Cerro Patacon andesites. Although the exact provenance of the material found in the Bas Obispo Formation is not known, large (up to boulder) clasts and immature sandstone deposits support a nearby Central Panamanian origin.
3) The Las Cascadas group includes dacitic pyroclastic density current deposits, dacitic fallout tuffs, flow-banded dacitic lava flows and rare dacitic dykes found between the southern Gatun Lake and new Pacific Locks area (Buchs et al., 2019). Volcanic deposits are found in the Las Cascadas, Culebra and Cucaracha Formations that were deposited in both terrestrial and marine environments during a transgressive regressive cycle in the Early Miocene (Kirby et al., 2008; Montes et al., 2012a). Volcanic deposits of the Las Cascadas group also occur in the La Boca Formation, which represents a shallow-marine, lateral analogue of the Cucaracha Formation in the new Pacific locks area (Buchs et al., 2019). These deposits reflect the development of proximal and distal composite volcanic centres of which the erosional

remnants can be found along the northern Gaillard Cut and other unstudied parts of Central Panama (Buchs et al., 2019). The tuffs, lavas and dykes of the Las Cascadas group have been dated between ca. 21 and 18 Ma (Fig. 2B) (Montes et al., 2012a; MacFadden et al., 2014; Bloch et al., 2016; Buchs et al., 2019; this study).

4) The Pedro Miguel group is predominantly composed of basalt to basaltic andesite tuffs with large basaltic intrusions, dykes, and rare gabbros and basaltic lava flows (Buchs et al., 2019; Farris et al., 2017; Montes et al., 2012a). This unit corresponds to the Pedro Miguel Formation that rests on top of, and is locally interbedded with, the other units of the Canal area (Buchs et al., 2019; Farris et al., 2017; Montes et al., 2012a). Because of geochemical and age similarity with the rest of the Pedro Miguel Formation, we include in this group mingled microgranodiorites and andesites from the Pacific entrance of the Canal that were previously included in the informal Panama City Formation (Farris et al., 2017). The "Panama City" terminology is not followed here due to the undefined age and stratigraphy of this unit, as well as geochemical diversity of its igneous rocks. The Pedro Miguel group corresponds to a field of monogenetic volcanoes in the form of tuff cones to tuff rings, with remarkable occurrences of km-sized subvolcanic peperitic intrusions (Buchs et al., 2019). We provide here the first geochronological data for this volcanism.

4.2. Petrography

The Cerro Patacon group is composed of andesites with abundant plagioclase and amphibole phenocrysts previously interpreted to reflect mineral accumulation in a water-saturated magma (Rooney et al., 2011). The Bas Obispo group includes clasts of porphyritic basalt to basaltic andesite with clinopyroxene and plagioclase phenocrysts (Fig. 3, Table S1). Phenocryst-melt disequilibrium is suggested by multiple zoning and resorption textures of the crystals, as well as high percentage of phenocrysts. Unlike previous work (Farris et al., 2017), amphibole was not encountered in our samples that have a whole rock composition similar to that previously reported for this unit. Alteration in the Bas Obispo group is generally high with abundant secondary clay minerals replacing the matrix.

The Las Cascadas group is predominantly composed of dacitic tuffs and lava flows with minor zoned plagioclase and broken clinopyroxene phenocrysts (Fig. 3, Table S1). The matrix of the lava flows is generally aphanitic and/or recrystalized, with shear planes in samples with flow banding. No amphibole was found in this group. Alteration in the Las Cascadas group is particularly high for the tuffs, with abundant secondary clay minerals replacing original vitric fragments, and poor preservation of the plagioclase phenocrysts.

Finally, the phenocrysts of the basaltic to basaltic andesitic igneous rocks of the Pedro Miguel group predominantly include plagioclase and pyroxene phenocrysts (Fig. 3, Table S1). Subvolcanic basalts, dolerites and gabbros have trachytic to subophitic textures, consistent with a tholeiitic crystallization series (Farris et al., 2017). Some samples include phenocrysts of olivine (generally altered) and low-Ca pyroxenes (enstatite to pigeonite) in addition to plagioclase and clinopyroxene. The Pacific entrance of the Canal includes unusual microgranodiorite and andesite with a mingling texture (Fig. 8A in Farris et al., 2017). Accidental clasts in the tuffs of the Pedro Miguel group include shallow- marine fossils and brown amphibole. The tuffs are pervasively altered with abundant secondary clay minerals replacing the original glass, and limited preservation of plagioclase and clinopyroxene phenocrysts. The basalt, gabbro, microgranodiorite and andesite are much better preserved than the tuff, with alteration predominantly occurring in interstitial glass and olivine phenocrysts.

4.3. Geochronology

A dacitic dyke of the Las Cascadas group was dated ca. 21 Ma in the southern Gatun Lake based on plagioclase (20.62 ± 0.06 Ma) and groundmass (21.51 ± 0.04 Ma) (Table 1). This dyke crosscuts coarse volcanic breccias of unclear origin, and extends the reach of the Las Cascadas group approximately 8 km to the west of its previously-documented occurrence. The Pedro Miguel group is dated here for the first time between 17.97 ± 0.11 and 16.90 ± 0.08 Ma based on plagioclase and groundmass (Table 1). Six ages are provided between Gatun Lake and the Pacific entrance of the Canal (i.e., a 30 km-long transect, Supplementary Fig. S1). These results are consistent with stratigraphic continuity of the Pedro Miguel Formation with the late Las Cascadas group dated in the Cucaracha Formation ca. 18 Ma (Fig. 2B) (Buchs et al., 2019). These geochronological constraints, together with field observations and geochemical data (see below), clearly establish the regional occurrence of the Pedro Miguel group above the Las Cascadas group. Significantly, new geochronological data also suggest that the duration of emplacement of the Pedro Miguel group was very short (approximately 1 m.yr.).

4.4. Whole rock geochemistry

Each of the four geochemical groups is characterised by distinct immobile trace element contents (Fig. 4). Differentiation is consistent within each group, as notably illustrated in a Nb/Y vs Zr/Ti classification diagram (Fig. 4A; Winchester and Floyd, 1977) and a TAS diagram (Fig. 5, based on samples with LOI <4 wt%). The groups can be further discriminated using a La/Sm vs Nb/Th diagram (Fig. 4B). In this diagram, the Bas Obispo basalts to basaltic andesites have lower Nb/Th at a given La/Sm compared to the other groups. Basalts and basaltic andesites of the Pedro Miguel group have higher Nb/Th and low La/Sm. The andesites of the Cerro Patacon group and the dacitic igneous rocks of the Las Cascadas group have a similar, higher La/Sm content compared to the Bas Obispo and Pedro Miguel groups. Unlike previous observations based on INAA and XRF data (Farris et al., 2011, 2017), immobile trace element patterns of the Cerro Patacon and Las Cascadas groups that are based on ICP-MS data show very similar characteristics (Fig. 4C-E). However, consistent with petrographic observations, the Las Cascadas group can be differentiated from the Cerro Patacon group based on a higher differentiation index (Zr/Ti in Fig. 4A) and SiO_2 content (Fig. 5A). Higher contents in trace elements in the Las Cascadas group relative to the Cerro Patacon group are consistent with the dacitic and andesitic composition of these groups, respectively. In normalised multielement diagrams (Fig. 4C-F) all groups have supra-subduction affinities with Nb and Ti negative anomalies.

In a TAS diagram all groups plot in the subalkaline field (Fig. 5A). The SiO_2 content of fresher samples is consistent with the Zr/Ti differentiation index in the Winchester and Floyd (1977) classification diagram (Fig. 4A). In a SiO_2 vs FeOt/MgO diagram the Cerro Patacon and Bas Obispo groups plot in the low-Fe to medium-Fe fields, whereas the Las Cascadas and Pedro Miguel groups plot in the medium-Fe to high-Fe fields (Fig. 5B; Arculus, 2003). In an AFM diagram, the Cerro Patacon and Bas Obispo groups plot in the calc-alkaline field, whereas the Las Cascadas and Pedro Miguel groups plot in the tholeiitic field (Fig. 5C). These characteristics show that the Las Cascadas and Pedro Miguel groups represent tholeiitic series, whereas the Cerro Patacon and Bas Obispo groups represent calc-alkaline series. This fundamental observation is consistent with our petrographic constraints and tholeiitic indexes calculated based on the relative decrease/increase of FeOt with decreasing MgO in these magmatic series (Farris et al., 2017). Our results also show that, when altered samples are discarded, the recognition of tholeiitic series in Central Panama is best achieved using an AFM diagram. Selected immobile and mobile trace elements confirm the distinctiveness of the geochemical groups (Fig. 6). In a Nb/Yb vs Th/Yb (Pearce, 2008) and Nb/Yb vs Ba/Yb diagrams, the Pedro Miguel group includes a few samples with unique geochemical affinities (i.e., partly lower Th/Yb and Ba/Yb at a given Nb/Yb) relative to other igneous rocks of the Canal area and other arc sequences in Panama (Fig. 6A-B). However, our results, which are based on ICP-MS data and only consider fresher samples for mobile elements, do not reproduce the trends previously presented for the igneous rocks in the Canal area (Farris et al., 2011, 2017). Unlike previous suggestion of an abrupt compositional change in Central Panama ca. 23 Ma (Farris et al., 2011), our data show significant compositional overlaps between geochemical groups of the Canal and other volcanic fronts in Panama. The only clear exception to this is the Ti content that is higher in the Las Cascadas and Pedro Miguel groups at a given SiO_2 content (Fig. 6F).

4.5. Clinopyroxene geochemistry

In the Canal area, where tuffs are frequently altered, and magma mixing is suggested by petrographic observations (e.g., rounded phenocrysts) and field observations (e.g., mingling textures), the analysis of unaltered clinopyroxenes can offer a valuable insight into the petrology and tectonic affinities of volcanic units.

All clinopyroxenes considered in this study (n=555) have an augite to diopside composition (Fig. 7B). Clinopyroxene-liquid equilibrium was tested using a simple Mg# equilibrium calculation, assuming $K_D(Fe\text{-}Mg)^{cpx\text{-}liq} = 0.28 \pm 0.08$ (Putirka, 2008), and using whole rock composition as an estimate of liquid composition (Fig. 7B). This approach shows that clinopyroxenes of the Bas Obispo group have a Mg# of ~75 in apparent equilibrium with their host rock of basaltic to basaltic andesitic compositions. Most of Pedro Miguel clinopyroxenes have a Mg# of ~70 also in apparent equilibrium with their host rock of basaltic to basaltic andesitic compositions. One exception to this are clinopyroxenes with an Mg# of ~53 from andesite sample DJ17–005, which represents a mingled component within a microgranodiorite in the Pacific entrance of the Canal. However, these clinopyroxenes are also in apparent equilibrium with their host rock. Most of Las Cascadas clinopyroxenes have an Mg# of ~70 similar to that of augites in the Pedro Miguel group. However, Las Cascadas augites are in clear disequilibrium with their host rocks of dacitic composition. Sample D16–021 of Las Cascadas group is an unusual rhyolitic clast in a dacitic tuff, which includes out-of-equilibrium clinopyroxenes with an Mg# of ~55. These are significant observations that reveal that the predominantly dacitic Las Cascadas group includes ubiquitous clinopyroxenes inherited from basaltic melts. These melts have so far not been directly observed (as whole rock) in this felsic group. In addition, clinopyroxenes from the Bas Obispo formation that are in apparent compositional equilibrium with their host rocks have a clear out-of-equilibrium crystal habits (Fig. 3A). Therefore, it is likely that many clinopyroxenes in apparent geochemical equilibrium with their host rock were in fact inherited during magma mixing, but this mixing is not revealed by equilibrium calculations based on Mg# alone. A similar observation was recently made using a multi-component equilibrium modelling of clinopyroxenes in Icelandic tholeiites (Neave and Putirka, 2017).

The empirical approach of Leterrier et al. (1982) was used to characterise possible alkaline, tholeiitic (MORB-like), tholeiitic (supra-subduction) and calc-alkaline affinities of magmatic series. A sample of sandstone from the Chagres-Bayano Arc with fresh detrital clinopyroxenes was also analysed for comparison with this older (pre- Oligocene) volcanic front of Central Panama. Augites with Mg# <65 that show evidence for Ti fractionation due to coeval ilmenite crystallization were not considered (i.e., samples D16–021 and DJ17–005 in Fig. 7C). Results of this approach, shown in Ca+Na vs Ti, Ca vs Ti+Cr and Al vs Ti diagrams (Leterrier et al., 1982), reveal fundamental differences between the clinopyroxene populations of the Bas Obispo, Las Cascadas and Pedro Miguel groups (Fig. 7D-F). Clinopyroxenes of the calc-alkaline Bas Obispo group have typical volcanic arc affinities, but fall in both the tholeiitic and calc-alkaline fields. The Bas Obispo clinopyroxenes with tholeiitic supra-subduction affinities closely resemble those from the Chagres-Bayano Arc sandstone. In contrast, none of the pyroxenes from the tholeiitic Las Cascadas and Pedro Miguel groups overlap with the Chagres-Bayano Arc pyroxenes. Instead, many of the Las Cascadas and Pedro Miguel clinopyroxenes fall in the calc-alkaline field in the Al vs Ti diagram (Fig. 7F). However, it is significant to note that the Las Cascadas and Pedro Miguel clinopyroxenes do not plot in the centre of the main calc-alkaline density envelopes defined by Leterrier et al. (1982), and do not overlap with calc-alkaline-like pyroxenes of the Bas Obispo group. This suggests that clinopyroxenes of the Las Cascadas and Pedro Miguel groups have an unusual composition not included in the original calibration of the discrimination diagrams of Leterrier et al. (1982). This interpretation is also supported by the unexpected composition of the other clinopyroxenes of the Las Cascadas and Pedro Miguel groups, which do not plot in the volcanic arc fields. Instead, a large fraction of these pyroxenes plot in the tholeiitic (non-orogenic or MORB-like) field, with a minor fraction of clinopyroxenes from the Pedro Miguel group in the alkaline field. Similar trends can be observed for pyroxenes in individual samples (Supplementary File 2), which indicates that the compositional variability of clinopyroxenes observed in the Leterrier et al. diagrams (Fig. 7) is not related to intrinsic volcanic and/or magmatic differences between the samples. Given the narrow Mg# range of the clinopyroxenes, and disequilibrium observations above, this variability is best explained by compositional differences in parental melts that have mixed on the way to the surface. Overall, these results confirm that unusual melting conditions were present in Central Panama during the formation of the Las Cascadas and Pedro Miguel groups.

5. Discussion

5.1. Geochemical and temporal evolution of the Panama volcanic arc

The Panama volcanic arc has undergone several phases of formation since its initiation in the Late Cretaceous (ca. 73 Ma, Buchs et al., 2010), which provide significant contextual information on the origin of volcanism in the Canal area. The first phase of magmatism following subduction initiation in Panama corresponds to formation of an early volcanic arc between the Campanian and Eocene, which is preserved and exposed today in the Azuero-Sona and Chagres-Bayano extinct arcs (Buchs et al., 2010; Maury et al., 1995; Montes et al., 2012a; Wegner et al., 2011) (Fig. 1). Compiled geochemical and geochronological data provide good control on the regional extent of the early volcanic front between ca. 70 and 40 Ma (Figs. 1–2). Geochemical data from Central Panama (Montes et al., 2012b; Wegner et al., 2011) indicate that the Chagres-Bayano Arc is composed of calc-alkaline and tholeiitic series that can be distinguished from the more recent volcanic arc by a relative depletion in the most incompatible trace elements (Figs. 4, 6). The Chagres-Bayano Arc also includes high-Mg basalts (Mg#=60–76), which have been dated between the Paleocene and Eocene (Wegner et al., 2011). These basalts do not seem to correspond to a short phase of development of the arc (Ar-Ar ages of 65.5 ± 1.6 and 49.4 ± 1.0 Ma; Wegner et al., 2011), but form a distinct geochemical group in various compositional spaces (Fig. 5). High-Mg basalts of the Chagres-Bayano Arc mostly plot in the tholeiitic field of the AFM diagram (Fig. 5C). These basalts could therefore be related to tholeiitic arc-like clinopyroxenes analysed in a sandstone from the Chagres area (Fig. 7). Volcanism studied in the Canal area does not overlap in time with the early activity of the Panama volcanic arc, and little geochemical overlap exists between the Chagres-Bayano Arc and geochemical groups of the Canal (Figs. 4–6). This demonstrates that volcanism in the Canal area records a distinct (younger) phase of magmatism, in a possibly distinct tectono-magmatic setting (Fig. 8).

Younger (post-Eocene) magmatism of the Panama volcanic arc predominantly consists of calc-alkaline series with an enrichment in the most incompatible trace elements relative to the older (pre-Oligocene) volcanic arc (Wegner et al., 2011) (Figs. 4, 6). The extent and duration of the post-Eocene magmatism is well constrained in Western Panama, where it forms the Central Cordillera Arc ("Cordilleran Arc" of Wegner et al., 2011) dated between ca. 34 and 5 Ma (Baker et al., 2016; Lissinna, 2005; Wegner et al., 2011) (Figs. 1–2). Several phases of magmatism could have occurred during this time interval in Western Panama due to, e.g., subduction of seamounts and changes in subduction dynamics (Gazel et al., 2015; Whattam and Stern, 2016). However, our compiled dataset, based on data from Wegner et al. (2011), Whattam et al. (2012) and Baker et al. (2016), does not reveal significant compositional changes between ca. 34 and 5 Ma, including at the proposed time of magmatic cessation in Central Panama ca. 16 Ma. As noted before (Whattam and Stern, 2016), resolution of the detailed evolution of the arc remains hampered by limited temporal control in large parts of Panama. Although the post-Eocene magmatic phase clearly overlaps in time with volcanism in the Canal area, the exact timing of the migration of volcanism from the old to young volcanic fronts in Western Panama is poorly constrained due to limited sampling and dating during the 40 to 30Ma time interval (Fig. 2). In addition, very limited information exists on the young volcanic front(s) in Eastern Panama apart from the Majé Range (ca. 20 Ma; Whattam et al., 2012); only few geochemical and geochronological data are available for the Pearl Islands and Sapo Range (ca. 22 to 18 Ma; Lissinna, 2005). Poor sampling of Eastern Panama means that it remains unclear whether the volcanic evolution of this area mirrors that of Western Panama or whether it was affected by a volcanic gap between ca. 40 and 22 Ma (Figs. 1–2). Detrital zircons collected in rivers of the San Blas Cordillera do not record ages younger than ca. 40 Ma (Ramirez et al., 2016), thus supporting volcanic intrusive cessation of this volcanic front at this time. However, it is unknown whether volcanism slowed down or fully stopped in Eastern Panama between the end of magmatism in the San Blas Cordillera (ca. 40 Ma) and younger magmatism south to this Cordillera (ca. 22 Ma). Significantly, the absence of active volcanism and apparent lack of post-18 Ma magmatism in Eastern Panama suggest that, unlike Western Panama, the eastern segment of the arc became extinct during the Miocene (Fig. 8).

Although the cause(s) of the migration of volcanic fronts in Panama between ca. 40 and 34 Ma remains poorly understood, it can be noted that this migration occurred following: (i) regional uplift event(s) in the Eocene (Mann and Kolarsky, 1995; Buchs et al., 2011; Montes et al., 2012a; Barat et al., 2014; Ramirez et al., 2016; Brandes and Winsemann, 2018); and (ii) initiation of oroclinal bending and associated development of the central Panamanian fault zone (Montes et al., 2012b) (Fig. 2). This suggests that relocation of magmatism in Panama resulted from a combination of changes in subduction dynamics possibly due to a reorganisation of plate tectonics in the Pacific (Brandes and Winsemann, 2018; Buchs et al., 2011), and collision of the Panama volcanic arc with South America in the Eocene (Barat et al., 2014). Another hypothesis that could explain reorganisation of arc fronts in the Late Eocene is the collision of an "indentor" (e.g., oceanic plateau) ca. 40 Ma (Whattam et al., 2012), but such an indentor has not yet been documented in accretionary complexes exposed along the Panamanian forearc (e.g., Buchs et al., 2011). Crucially, volcanism of the

Panama Canal (ca. 25 to 16 Ma) postdates migration of the volcanic front (ca. 40 to 34 Ma) (Fig. 2), therefore suggesting that this volcanism represents a distinct magmatic phase (Fig. 8).

The most recent phase of development of the Panama volcanic arc is documented by alkaline basalts and adakites younger than ca. 5 Ma, which occur over most of Western Panama and are associated with modern (dormant) volcanic centres (Abratis and Wörner, 2001; Defant et al., 1992; Gazel et al., 2011) (Figs. 1–2). This alkaline and adakitic magmatic phase has been associated with the collision of the Cocos Ridge, subduction of the Cocos-Nazca plate boundary and/or formation of a slab window in Western Panama. Although adakitic volcanism could have occurred before 5Ma, "adakitic-like" magmatism that was suggested to occur in Central and Eastern Panama between approximately 30 and 19 Ma (Whattam et al., 2012) is compositionally undistinguishable from other non-adakitic arc magmatism in the same time interval in Western Panama (Baker et al., 2016), and therefore was considered here to be part of our post-Eocene arc group (Fig. 2). The composition of post-5 Ma adakites and alkaline basalts in Western Panama indicates that this young volcanic phase has no known equivalent in the earlier history of the arc, including volcanism of the Panama Canal (Figs. 4–6).

In summary, regional constraints show that volcanism in the Canal area between ca. 25 to 16 Ma: (i) postdates early (pre-32 Ma) deformation and faulting of Central Panama; (ii) was coeval with magmatism in Western Panama (Cordilleran phase sensu Wegner et al., 2011) and Eastern Panama; and (iii) shortly postdates the youngest known magmatic activity in Eastern Panama ca. 18 Ma. We show below that this volcanism can be accounted for by a simple model of regional magmatic shutdown in response to breakup of the Farallon plate.

5.2. Volcanic shutdown in Central Panama

Magmatic activity in the Canal area has previously been associated with rifting of Central Panama due to collision of the Panama volcanic arc with South America ca. 23 Ma (Farris et al., 2011, 2017).Two key observations support this interpretation: (i) a change of magmatism from hydrous to anhydrous melting ca. 23 Ma, supported by the appearance of tholeiitic volcanism in the Canal area and a depletion in large ion lithophile elements (LILE) relative to pre-23 Ma volcanism in Panama; and (ii) a regional uplift ca. 23 Ma supported by thermochronological data, and interpreted to result from arc-continent collision. However, whole rock geochemical observations show that, apart from tholeiitic affinities and a higher Ti content of the Las Cascadas and Pedro Miguel groups, there is no significant difference between the Canal area and the post-Eocene (34 to 5 Ma) arc in Panama (in particular when the full compositional range of the recent arc is taken into account, Figs. 4–6). In addition, temporal correlation between volcanic activity of the Canal area and the collision between Panama and South America is still poorly constrained. Proposed ages of collision range between the Late Cretaceous (Kennan and Pindell, 2009; Pindell, 1993), Eocene (Barat et al., 2014), Oligocene-Miocene (Farris et al., 2011) and Miocene (Coates et al., 2004; Duque-Caro, 1990; Montes et al., 2012b; Montes et al., 2015). Although Central Panama includes a complex fault system thought to have segmented the old volcanic front since ca. 40–32 Ma (Barat et al., 2014; Mann and Kolarsky, 1995; Montes et al., 2012a, 2012b; Stewart et al., 1980), there is yet no evidence for significant extension and rifting in the Canal area between the Oligocene and Miocene. Volcaniclastic and sedimentary deposits in this area could have easily been accommodated in topographic lows between volcanic centres in the Central Panama Volcanic Field (Buchs et al., 2019). Also, regional thermochronological data (Montes et al., 2012a; Ramírez et al., 2016) and geological data (Barat et al., 2014; Buchs et al., 2011; Mann and Kolarsky, 1995; Montes et al., 2012a) do not outline a clear ca. 23 Ma tectonic event. These data support instead a complex series of regional and local uplifts between the Eocene and Miocene, for which relative contribution from subduction tectonics and arc-continent collision is difficult to unravel. In contrast, there is a clear overlap between breakup of the Farallon plate ca. 23 Ma (Barckhausen et al., 2008; Lonsdale, 2005) and magmatic changes in the Canal area, which strongly suggests a causal relationship between these two processes (Fig. 8).

Breakup of the Farallon plate into the Cocos and Nazca Plates ca. 23 Ma is, arguably, the most significant tectonic event during the evolution of the Panama volcanic arc since the Late Cretaceous. Although tectonic reconstructions in the Eastern Pacific are limited by subduction of the Lower Miocene oceanic crust originally produced at the Cocos- Nazca Spreading Centre, initiation of this spreading could have been associated with a change from orthogonal convergence between the Farallon and Caribbean plates to oblique convergence between the Nazca and Caribbean Plates (Lonsdale, 2005; Lonsdale and Klitgord, 1978; Meschede et al., 2008; Morell, 2015). Local change to a strike-slip margin ca. 23 Ma could have progressively reduced the water supply in the subduction zone, which we propose led to magmatic shutdown by suppression of hydrous melting of Central and possibly Eastern Panama in the Miocene (ca. 16 Ma), without a significant change in trace element contents relative to the coeval post-Eocene arc in Western Panama. Although considerable uncertainties exist on the tectonic evolution of the convergent margin in Panama in the Early Miocene, reduction of orthogonal convergence between the Nazca and Caribbean Plates in Central and Eastern Panama (but not along the magmatically active Western Panama) could also have been facilitated by counterclockwise rotation of the subduction zone during oroclinal bending of the volcanic arc (Barat et al., 2014; Mann and Corrigan, 1990; Montes et al., 2012b; Silver et al., 1990), as illustrated in Fig. 8.

Magmatic shutdown in Central Panama in the Early Miocene is in very good agreement with our new temporal and geochemical constraints from the Canal area. Calc-alkaline magmatism of the Bas Obispo and Cerro Patacon groups (ca. 25 to 24 Ma) and younger tholeiitic magmatism of the Las Cascadas and Pedro Miguel groups (ca. 21 to 16 Ma) are consistent with a change from hydrous to anhydrous magmatism ca. 23 Ma (Fig. 5). A change from hydrous to anhydrous melting was previously associated with disappearance of amphibole ca. 23 Ma (Farris et al., 2017). However, our petrographic and SEM observations do not document the presence of amphibole in the calc-alkaline series of the Bas Obispo group (ca. 25 to 24 Ma). This is consistent with the hypothesis that amphibole preservation was predominantly controlled by water saturation in melts during crustal storage and ascent (e.g., Rooney et al., 2011), rather than water content in the melting region. However, transition from calc-alkaline to tholeiitic volcanism ca. 23 Ma is also well supported by the clinopyroxene cargo that shows that parental melts (Mg# of ~50) of the Las Cascadas and Pedro Miguel groups have unusual MORB-like and alkaline/transitional affinities not observed in earlier magmatic phases (Fig. 7). Although dacitic melts of Las Cascadas group could have been produced by crustal assimilation in tholeiitic melts (Farris et al., 2017), compositional differences between the Las Cascadas and Pedro Miguel clinopyroxenes reveal that distinct parental melts were involved in the formation of these groups. Unravelling the exact nature and composition of these melts would require a detailed petrological analysis that is beyond the scope of this study.

Pyroxene geochemistry additionally documents an apparent increase in alkalinity of parental melts from the Las Cascadas group (ca. 21 to 18 Ma) to the Pedro Miguel group (ca. 18 to 16 Ma) (Fig. 7C-D, based on Ti proxy). Consistently with magmatic waning of Central Panama shortly after ca. 23 Ma, this observation suggests an increase in the depth of mantle partial melting concurrent with the development of anhydrous melting conditions. This secular change could also be associated with the appearance of higher Ti content in the post-23 Ma Las Cascadas and Pedro Miguel groups (Fig. 6F). Interestingly, this type of secular change is similar to that of some Pacific oceanic islands, where increased alkalinity typically accompanies magmatic shutdown (e.g., Clague and Dalrymple, 1987). However, unambiguous alkaline melts have not been encountered yet in the Canal area, where extensive magma mixing could in fact obscure recognition of this component. In any case, a secular change of the Canal magmatism is also consistent with lower Th/Yb and Ba/Yb ratios in some whole rock samples of the Pedro Miguel group (Fig. 6), which likely reflect decreasing contribution of slab components shortly before magmatic shutdown ca. 16 Ma.

The development of the transisthmian fault system has been associated with a complex interplay of normal, strike-slip and thrust faults (e.g., Mann and Corrigan, 1990; Montes et al., 2012a; Rockwell et al., 2010a, 2010b; Schug et al., 2018; Stewart et al., 1980). However, interpretation of the fault kinematics is hampered by limited exposures in Central Panama, and kinematics of the major faults have been interpreted in different ways in different studies. Therefore, it is currently not possible to determine whether (and where) extension occurred in Central Panama, and whether this extension was sufficient to create decompression melting of the subarc asthenosphere as hypothesized in Farris et al. (2011). However, deformation in Central Panama was most likely associated with the formation of deep-rooted, lithospheric faults that contributed to dismemberment of ancient volcanic fronts ca. 40 to 32Ma (Barat et al., 2014; Montes et al., 2012b). We propose here that the occurrence of these faults could have promoted melt extraction in the Canal area ca. 25 to 16 Ma (Fig. 8). The unusual occurrence of faulted (and possibly locally thinner) crust in Central Panama could explain why there is no other documented analogue of the atypical post-23 Ma tholeiitic magmatism seen in the Canal area (in the absence of a full published dataset, we could not assess whether the Valiente

Formation in Western Panama mentioned in Farris et al., 2011 could represent a possible analogue). Volcanic and/or petrological effects of lithospheric faulting in Central Panama could also have predated breakup of the Farallon plate. A possible hint for this effect is given by whole rock trace element contents of the Bas Obispo group that, despite a ca. 25 to 24 Ma age, are intermediate between the pre-Oligocene and post-Eocene volcanic arcs in La/Sm vs Nb/Th and primitive mantle normalised multielement diagrams (Fig. 4b, d). This suggests that the more depleted mantle components associated with the pre-Oligocene volcanic arc (Wegner et al., 2011) could have survived migration of the volcanic front ca. 41–34 Ma, and were tapped into and remained unmixed on their way to the surface because of facilitated extraction along deep-rooted faults. Overall, this suggests that magmatic shutdown could have occurred synchronously (?) between Central and Eastern Panama in the Early Miocene (Fig. 8), but has not been yet documented regionally because of inherent difficulties in extracting and preserving lower-volume melts associated with this event.

6. Conclusions

Magmatism preserved in Central Panama is interpreted as a particular record of magmatic shutdown following breakup of the Farallon plate. Four main magmatic groups are recognised in the Canal area, which have trace element affinities generally like those of the recent (post-Eocene) phase of cordilleran volcanic activity between Western and Eastern Panama. However, the composition of clinopyroxenes phenocrysts coupled with a change from calc-alkaline to tholeiitic whole rock affinities in the Canal area reveal that significant petrological changes occurred in Central Panama between ca. 25 and 16 Ma. These changes are consistent with suppression of water in the subduction zone and waning of magmatism ca. 16 Ma, after that subduction became more oblique following the breakup of the Farallon plate ca. 23 Ma. Given a large range of regional and local constraints, volcanism in the Canal area is unlikely to have been directly induced by extension in Central Panama. Instead, early development of a transisthmian fault zone in this area (ca. 40–32 Ma, synchronous to migration of volcanic fronts in Panama) could have facilitated extraction of unusual melts associated with magmatic shutdown in the Early Miocene. A similar evolution could have occurred in Eastern Panama, leading to suppression of volcanism until present, but this hypothesis remains to be tested with additional work in this poorly studied area.

Previous regional constraints and new data from the Central Panama Volcanic Field show that the topography of Central Panama reflects a complex interplay of tectonic and volcanic processes, including: (i) formation of a prominent pre-40 Ma volcanic front (Azuero-Sona and Chagres-Bayano arc); (ii) development of a transisthmian fault system since 40–32 Ma due to possible collision of the Panama volcanic arc with South America; (iii) migration of volcanic fronts of the Panama arc in the Eocene-Oligocene; and (iv) magmatic shutdown in the Early Miocene. Without the combination of pre-Miocene arc segmentation and volcanic cessation ca. 16 Ma, it is unlikely that a low topography could have developed and survived in Central Panama. Magmatic cessation in this area was most likely key to preventing obstruction by prominent volcanic centres, similar to El Valle volcano at the eastern termination of the Central Cordillera. Therefore, magmatic cessation was essential in establishing the unique natural environment of Central Panama. It also played a significant role in providing topographic conditions required for successful building of the Panama Canal. Overall our study shows that improving our understanding the volcanic evolution of southern Central America and its link to tectonics will be essential for reconstructing the palaeogeographic evolution of the region and, particularly, closure of the last interoceanic straits associated with final emergence of the Panama Isthmus.

Supplementary data to this article can be found online at https://doi.org/10.1016/j.lithos.2019.02.016.

Acknowledgment

This manuscript benefited from constructive criticism from Scott Whattam and an anonymous reviewer. We are grateful to Stewart Redwood for his comments on the manuscript and numerous discussions on the geology of Panama over the past few years. We also thank Iain McDonald and Duncan Muir at Cardiff University, and Dan Higgins at OSU Argon Geochronology Laboratory for analytical support. This study was supported by funds from the Panama Canal Authority, grant #GEFNE137-15 of the National Geographic Society, 202 D.M. Buchs et al. / Lithos 334–335 (2019) 190–204 grant #201606400067 of the China Scholarship Council and matching funds from Cardiff University.

References

Abratis, M., Wörner, G., 2001. Ridge collision, slab-window formation, and the flux of Pacific asthenosphere into the Caribbean realm. Geology 29, 127–130. https://doi.org/ 10.1130/0091-7613(2001)029b0127:rcswfaN2.0.co;2.

Arculus, R.J., 2003. Use and abuse of the terms calcalkaline and calcalkalic. Journal of Petrology 44, 929–935.

Bacon, C.D., Silvestro, D., Jaramillo, C., Smith, B.T., Chakrabarty, P., Antonelli, A., 2015. Biological evidence supports an early and complex emergence of the Isthmus of Panama. Proceedings of the National Academy of Sciences 112, 6110–6115. https://doi.org/10.1073/pnas.1423853112.

Baker, M.J., Hollings, P., Thompson, J.A., Thompson, J.M., Burge, C., 2016. Age and geochemistry of host rocks of the Cobre Panama porphyry Cu–au deposit, Central Panama: Implications for the Paleogene evolution of the Panamanian magmatic arc. Lithos 248–251, 40–54. https://doi.org/10.1016/j.lithos.2016.01.014.

Barat, F., Mercier de Lépinay, B., Sosson, M., Müller, C., Baumgartner, P.O., Baumgartner-Mora, C., 2014. Transition from the Farallon Plate subduction to the collision between South and Central America: Geological evolution of the Panama Isthmus. Tectonophysics 622, 145–167. https://doi.org/10.1016/j.tecto.2014.03.008.

Barckhausen, U., Ranero, C.R., Cande, S.C., Engels, M., Weinrebe, W., 2008. Birth of an intraoceanic spreading center. Geology 36, 767–770. https://doi.org/10.1130/g25056a.1.

Bloch, J.I., Woodruff, E.D., Wood, A.R., Rincon, A.F., Harrington, A.R.,Morgan, G.S., Foster, D.A., Montes, C., Jaramillo, C.A., Jud, N.A., Jones, D.S., MacFadden, B.J., 2016. First north American fossil monkey and early Miocene tropical biotic interchange. Nature 533, 243–246. https://doi.org/10.1038/nature17415.

Brandes, C., Winsemann, J., 2018. From incipient island arc to doubly-vergent orogen: a review of geodynamic models and sedimentary basin-fills of southern Central America. Island Arc 0, e12255. https://doi.org/10.1111/iar.12255.

Buchs, D.M., Arculus, R.J., Baumgartner, P.O., Baumgartner-Mora, C., Ulianov, A., 2010. Late cretaceous arc development on the SW margin of the caribbean plate: insights from the Golfito, Costa Rica, and Azuero, Panama, complexes. Geochemistry Geophysics Geosystems 11, Q07S24. https://doi.org/10.1029/2009gc002901.

Buchs, D.M., Baumgartner, P.O., Baumgartner-Mora, C., Flores, K., Bandini, A.N., 2011. Upper cretaceous to Miocene tectonostratigraphy of the Azuero area (Panama) and the discontinuous accretion and subduction erosion along the Middle American margin. Tectonophysics 512, 31–46.

Buchs, D.M., Irving, D., Coombs, H., Miranda, R., Wang, J., Coronado, R., Arrocha, R., Lacerda, M., Goff, C., Almengor, E., Portugal, E., Franceschi, P., Chichaco, E., Redwood, S.R., 2019. Volcanic contribution to emergence of Central Panama in the early Miocene. Scientific Reports https://doi.org/10.1038/s41598-018-37790-2.

Clague, D.A., Dalrymple, G.B., 1987. The Hawaiian-Emperor volcanic chain, Part I, Geologic evolution. In: Decker, R.W., Wright, T.L., Stauffer, P.H. (Eds.), Volcanism in Hawaii, U.S. Geological Survey Professional Paper. U.S. Government Printing Office, pp. 5–54.

Coates, A.G., Collins, L.S., Aubry, M.P., Berggren, W.A., 2004. The geology of the Darien, Panama, and the late Miocene-Pliocene collision of the Panama arc with northwestern South America. Geological Society of America Bulletin 116, 1327–1344.

Collins, L.S., Coates, A.G., Berggren, W.A., Aubry, M.-P., Zhang, J., 1996. The late Miocene Panama isthmian strait. Geology 24, 687–690. https://doi.org/10.1130/0091-7613(1996)024b0687:tlmpisN2.3.co;2.

Defant, M.J., Jackson, T.E., Drummond, M.S., De Boer, J.Z., Bellon, H., Feigenson, M.D., Maury, R.C., Stewart, R.H., 1992. The geochemistry of young volcanism throughout western Panama and southeastern Costa Rica: an overview. Journal of the Geological Society 149, 569–579. https://doi.org/10.1144/gsjgs.149.4.0569.

Duque-Caro, H., 1990. The Choco block in the northwestern corner of South America: structural, tectonostratigraphic, and paleogeographic implications. Journal of South American Earth Sciences 3, 71–84. https://doi.org/10.1016/0895-9811(90)90019-W.

Farris, D.W., Jaramillo, C., Bayona, G., Restrepo-Moreno, S.A.,Montes, C., Cardona, A., Mora, A., Speakman, R.J., Glascock, M.D., Valencia, V., 2011. Fracturing of the Panamanian Isthmus during initial collision with South America. Geology 39, 1007–1010. https://doi.org/10.1130/g32237.1.

Farris, D.W., Cardona, A., Montes, C., Foster, D., Jaramillo, C., 2017. Magmatic evolution of Panama Canal volcanic rocks: a record of arc processes and tectonic change. PLoS One 12, e0176010. https://doi.org/10.1371/journal.pone.0176010.

Gale, A., Dalton, C.A., Langmuir, C.H., Su, Y., Shilling, J.-G., 2013. The mean composition of ocean ridge basalts. Geochemistry, Geophysics, Geosystems 14, 489–518. https://doi.org/10.1029/2012GC004334.

Gazel, E., Hoernle, K., Carr, M.J., Herzberg, C., Saginor, I., van den Bogaard, P., Hauff, F., Feigenson, M., Swisher III, C., 2011. Plume-subduction interaction in southern Central America: mantle upwelling and slab melting. Lithos 121, 117–134.
Gazel, E., Hayes, J.L., Hoernle, K., Kelemen, P., Everson, E., Holbrook, W.S., Hauff, F., van den Bogaard, P., Vance, E.A., Chu, S., Calvert, A.J., Carr, M.J., Yogodzinski, G.M., 2015. Continental crust generated in oceanic arcs. Nature Geoscience 8, 321–327. https://doi.org/10.1038/ngeo2392.
Haug, G.H., Tiedemann, R., 1998. Effect of the formation of the Isthmus of Panama on Atlantic Ocean thermohaline circulation. Nature 393, 673–676.
Keigwin, L., 1982. Isotopic paleoceanography of the Caribbean and East Pacific: role of panama uplift in late neogene time. Science 217, 350–353. https://doi.org/10.1126/science.217.4557.350.
Kennan, L., Pindell, J., 2009. Dextral shear, terrane accretion and basin formation in the Northern Andes: explained only by interaction with a Pacific-derived Caribbean Plate. In: James, K.H., Lorente, M.A., Pindell, J. (Eds.), The Origin and Evolution of the Caribbean Plate. Geological Society of London (Special Publication). The Geological Society of London, pp. 487–531.
Kirby, M.X., Jones, D.S., MacFadden, B.J., 2008. Lower miocene stratigraphy along the panama canal and its bearing on the central American Peninsula. PLoS One 3, e2791.
Kolarsky, R.A., Mann, P., Monechi, S., Meyerhoff, H.D., Pessagno, E.A., 1995. Stratigraphic development of southwestern Panama as determined from integration of marine seismic data and onshore geology; geologic and tectonic development of the Caribbean Plate boundary in southern Central America. In: Mann, P. (Ed.), Geologic and
Tectonic Development of the Caribbean Plate Boundary in Southern Central America. Geological Society of America Special Paper, pp. 159–200.
Koppers, A.A.P., 2002. ArArCALC—software for 40Ar/39Ar age calculations. Computers & Geosciences 28, 605–619. https://doi.org/10.1016/S0098-3004(01)00095-4.
Kuiper, K.F., Deino, A., Hilgen, F.J., Krijgsman, W., Renne, P.R., Wijbrans, J.R., 2008. Synchronizing Rock Clocks of Earth history. Science 320, 500–504.
Leterrier, J., Maury, R., Thonon, P., Girard, D., Marchal, M., 1982. Clinopyroxene composition
as a method of identification of the magmatic affinities of paleo-volcanic series. Earth and Planetary Science Letters 59, 139–154.
Lissinna, B., 2005. A Profile Though the Central American Landbridge in western Panama: 115 Ma Interplay Between the Galápagos Hotspot and the Central American Subduction Zone. Unpublished PhD thesis. Christian-Albrechts University, Kiel https://macau.uni-kiel.de/servlets/MCRFileNodeServlet/dissertation_derivate_00001612/d1612.pdf.
Lonsdale, P., 2005. Creation of the Cocos and Nazca plates by fission of the Farallon plate. Tectonophysics 404, 237–264.
Lonsdale, P., Klitgord, K.D., 1978. Structure and tectonic history of the eastern Panama Basin. Geological Society of America Bulletin 89, 981–999. https://doi.org/10.1130/0016-7606(1978)89b981:sathotN2.0.co;2.
MacFadden, B.J., Bloch, J.I., Evans, H., Foster, D.A., Morgan, G.S., Rincon, A., Wood, A.R., 2014. Temporal Calibration and Biochronology of the Centenario Fauna, early Miocene of Panama. The Journal of Geology 122, 113–135. https://doi.org/10.1086/675244.
MacFadden, B.J., Jones, D.S., Jud, N.A., Moreno-Bernal, J.W., Morgan, G.S., Portell, R.W., Perez, V.J., Moran, S.M., Wood, A.R., 2017. Integrated chronology, flora and faunas, and paleoecology of the Alajuela Formation, late Miocene of Panama. PLoS One 12. https://doi.org/10.1371/journal.pone.0170300.
Mann, P., Corrigan, J., 1990. Model for late Neogene deformation in Panama. Geology 18, 558–562. https://doi.org/10.1130/0091-7613(1990)018b0558:mflndiN2.3.co;2.
Mann, P., Kolarsky, R.A., 1995. East Panama deformed belt: structure, age, and neotectonics significance. In: Mann, P. (Ed.), Geologic and Tectonic Development of the Caribbean Plate Boundary in Southern Central America. vol. 295. Geological Society of America Special Paper, pp. 111–130.
Marshall, L.G., Webb, S.D., Sepkoski, J.J., Raup, D.M., 1982. Mammalian evolution and the great American interchange. Science 215, 1351–1357. https://doi.org/10.1126/science.215.4538.1351.
Maury, R.C., Defant, M.J., Bellon, H., de Boer, Z.J., Stewart, R.H., Cotten, J., 1995. Early tertiary arc volcanics from eastern Panama: geologic and tectonic development of the Caribbean Plate boundary in southern Central America. In: Mann, P. (Ed.), Geologic and Tectonic Development of the Caribbean Plate Boundary in Southern Central America. vol. 295. Geological Society of America Special Paper, pp. 29–34.
Meschede, M., Barckhausen, U., Engels, M., Weinrebe, W., 2008. The trace of the Pacific-Cocos-Nazca triple junction in the Central Pacific and the formation of an overlapping spreading Centre. Terra Nova 20, 246–251. https://doi.org/10.1111/j.1365-3121.2008.00812.x.

Min, K., Mundil, R., Renne, P.R., Ludwig, K.R., 2000. A test for systematic errors in 40Ar/39Ar geochronology through comparison with U/Pb analysis of a 1.1-Ga rhyolite. Geochimica et Cosmochimica Acta 64, 73–98. https://doi.org/10.1016/S0016-7037(99)00204-5.

Montes, C., Cardona, A., McFadden, R., Morón, S.E., Silva, C.A., Restrepo-Moreno, S., Ramírez, D.A., Hoyos, N., Wilson, J., Farris, D., Bayona, G.A., Jaramillo, C.A., Valencia, V., Bryan, J., Flores, J.A., 2012a. Evidence for Middle Eocene and Younger Land Emergence in Central. Implications for Isthmus closure. Geological Society of America Bulletin, Panama https://doi.org/10.1130/b30528.1.

Montes, C., Bayona, G., Cardona, A., Buchs, D.M., Silva, C.A., Morón, S., Hoyos, N., Ramírez, D.A., Jaramillo, C.A., Valencia, V., 2012b. Arc-continent collision and orocline formation: closing of the central American seaway. Journal of Geophysical Research 117, B04105.

Montes, C., Cardona, A., Jaramillo, C., Pardo, A., Silva, J.C., Valencia, V., Ayala, C., Pérez-Angel, L.C., Rodriguez-Parra, L.A., Ramirez, V., Niño, H., 2015. Middle Miocene closure of the central American Seaway. Science 348, 226–229. https://doi.org/10.1126/science.aaa2815.

Morell, K.D., 2015. Late Miocene to recent plate tectonic history of the southern Central America convergent margin. Geochemistry, Geophysics, Geosystems 16, 3362–3382. https://doi.org/10.1002/2015GC005971.

Neave, D.A., Putirka, K.D., 2017. A new clinopyroxene-liquid barometer, and implications for magma storage pressures under Icelandic rift zones. American Mineralogist 102, 777–794. https://doi.org/10.2138/am-2017-5968.

O'Dea, A., Lessios, H.A., Coates, A.G., Eytan, R.I., Restrepo-Moreno, S.A., Cione, A.L., Collins, L.S., de Queiroz, A., Farris, D.W., Norris, R.D., Stallard, R.F.,Woodburne, M.O., Aguilera, O., Aubry, M.-P., Berggren, W.A., Budd, A.F., Cozzuol, M.A., Coppard, S.E., Duque-Caro, H., Finnegan, S., Gasparini, G.M., Grossman, E.L., Johnson, K.G., Keigwin, L.D., Knowlton, N., Leigh, E.G., Leonard-Pingel, J.S., Marko, P.B., Pyenson, N.D., Rachello-Dolmen, P.G., Soibelzon, E., Soibelzon, L., Todd, J.A., Vermeij, G.J., Jackson, J.B.C., 2016. Formation of the Isthmus of Panama. Science Advances 2. https://doi.org/10.1126/sciadv.1600883.

Pearce, J.A., 2008. Geochemical fingerprinting of oceanic basalts with applications to ophiolite classification and the search for Archean oceanic crust. Lithos 100, 14–48.

Pindell, J.L., 1993. Regional synopsis of gulf of Mexico and Caribbean evolution. GCSSEPM Foundation 13th Annual Research Conference Proceedings, pp. 251–274 July 1.

Putirka, K., 2008. Excess temperatures at ocean islands: Implications for mantle layering and convection. Geology 36, 283–286. https://doi.org/10.1130/g24615a.1.

Ramírez, D.A., Foster, D.A., Min, K., Montes, C., Cardona, A., Sadove, G., 2016. Exhumation of the Panama basement complex and basins: Implications for the closure of the central American seaway. Geochemistry, Geophysics, Geosystems https://doi.org/10.1002/2016GC006289.

Rockwell, T., Gath, E., Gonzalez, T., Madden, C., Verdugo, D., Lippincott, C., Dawson, T., Owen, L.A., Fuchs, M., Cadena, A., Williams, P., Weldon, E., Franceschi, P., 2010a. Neotectonics and paleoseismology of the Limón and pedro miguel faults in Panamá: earthquake hazard to the Panamá canal. Bulletin of the Seismological Society of America 100, 3097–3129. https://doi.org/10.1785/0120090342.

Rockwell, T.K., Bennett, R.A., Gath, E., Franceschi, P., 2010b. Unhinging an indenter: a new tectonic model for the internal deformation of Panama. Tectonics 29, TC4027. https://doi.org/10.1029/2009tc002571.

Rooney, T., Franceschi, P., Hall, C., 2011.Water-saturatedmagmas in the Panama Canal region: a precursor to adakite-like magma generation? Contributions to Mineralogy and Petrology 161, 373–388. https://doi.org/10.1007/s00410-010-0537-8.

Schug, D.L., Salter, P., Goetz, C., Irving, D., 2018. Pedro Miguel Fault Investigations: borinquen Dam 1e Construction and the Panama Canal expansion. Environmental and Engineering Geoscience 24, 39–53. https://doi.org/10.2113/gseegeosci.24.1.39.

Silver, E.A., Reed, D.L., Tagudin, J.E., Heil, D.J., 1990. Implications of the North and South Panama thrust belts for the origin of the Panama Orocline. Tectonics 9, 261–281.

Steiger, R.H., Jäger, E., 1977. Subcommission on geochronology: convention on the use of decay constants in geo- and cosmochronology. Earth and Planetary Science Letters 36, 359–362. https://doi.org/10.1016/0012-821X(77)90060-7.

Stewart, R.H., Stewart, J.L., With Collaboration by Woodring, W.P, 1980. Geologic Map of the Panama Canal and Vicinity, Republic of Panama (Report no. 1232). US Geological Survey Publication.

Wegner, W., Wörner, G., Harmon, R.S., Jicha, B.R., 2011. Magmatic history and evolution of the central American Land Bridge in Panama since cretaceous times. Geological Society of America Bulletin 123, 703–724. https://doi.org/10.1130/b30109.1.

Whattam, S.A., Stern, R.J., 2016. Arc magmatic evolution and the construction of continental crust at the central American Volcanic Arc system. International Geology Review 58, 653–686. https://doi.org/10.1080/00206814.2015.1103668.

Whattam, S.A., Montes, C., McFadden, R.R., Cardona, A., Ramirez, D., Valencia, V., 2012. Age and origin of earliest adakitic-like magmatism in Panama: Implications for the tectonic evolution of the Panamanian magmatic arc system. Lithos 142-143, 226–244.

Winchester, J.A., Floyd, P.A., 1977. Geochemical discrimination of different magma series and their differentiation products using immobile elements. Chemical Geology 20, 325–343.

Wörner, G., Harmon, R.S., Hartmann, G., Simon, K., 2005. Igneous geology and geochemistry of the upper río chagres basin. In: Singh, V.P., Harmon, R.S. (Eds.), The Río Chagres, Panama: A Multidisciplinary Profile of a Tropical Watershed. Water Science and Technology Library, pp. 65–81.

Table 1
Geochronological results.

Sample	Lithology	Formation	Locality	Latitude	Longitude	Age (Ma, 2σ)		Preferred age
						Plagioclase	Groundmass	
DAT-2	Amygdaloidal basalt	Pedro Miguel	New Pacific locks	8.99477	−79.60182	–	17.97 ± 0.11	17.97 ± 0.11
DAT-3	Amygdaloidal basalt	Pedro Miguel	New Pacific locks	8.99484	−79.60188	–	16.90 ± 0.08	16.90 ± 0.08
DAT-4	Columnar basalt	Pedro Miguel	New Pacific locks	8.97819	−79.58510	17.20 ± 0.07	–	17.20 ± 0.07
DAT-6	Columnar basalt	Pedro Miguel	New Pacific locks	8.99635	−79.60287	–	17.20 ± 0.07	17.20 ± 0.07
DJ17-005	Mingled microgranodiorite	Pedro Miguel	Puente de las Americas	8.93909	−79.56561	–	16.48 ± 0.09	16.48 ± 0.09
DJ17-013	Basaltic andesite	Pedro Miguel	Isla Barbacoa	9.12081	−79.79585	–	16.75 ± 0.08	16.75 ± 0.08
DJ17-014	Dyke of dacite	Las Cascadas	Bordada Gamboa	9.11830	−79.75443	20.62 ± 0.06	21.51 ± 0.04	20.62 ± 0.06

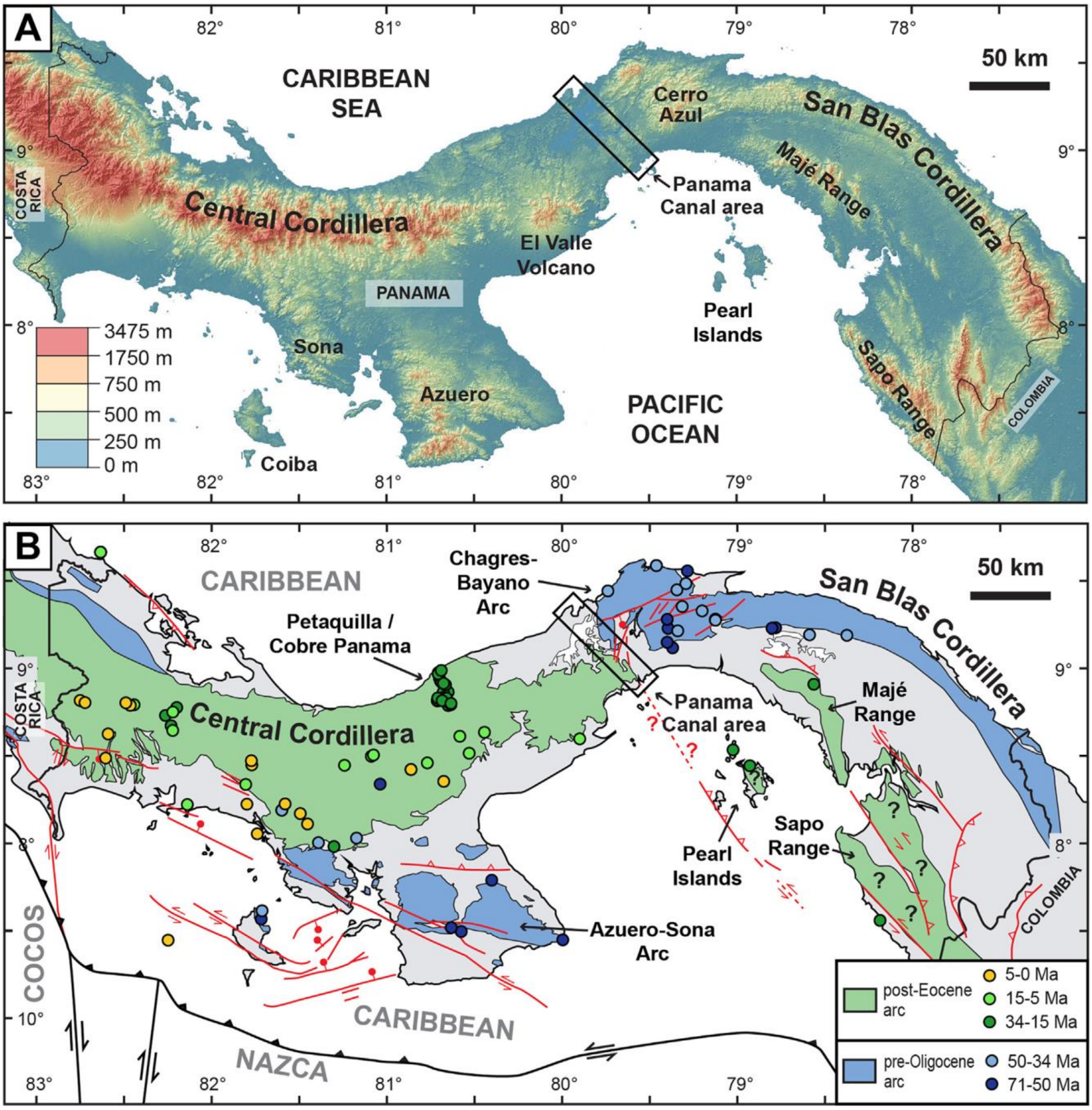

Fig. 1. Geological setting of Panama. (A) Digital topography model based on SRTM data from USGS Global Visualization Viewer tool (https://glovis.usgs.gov/, retrieved online in 2017). (B) Simplified geological map modified from Buchs et al. (2010). The source of geochronological data is given in the Methods section.

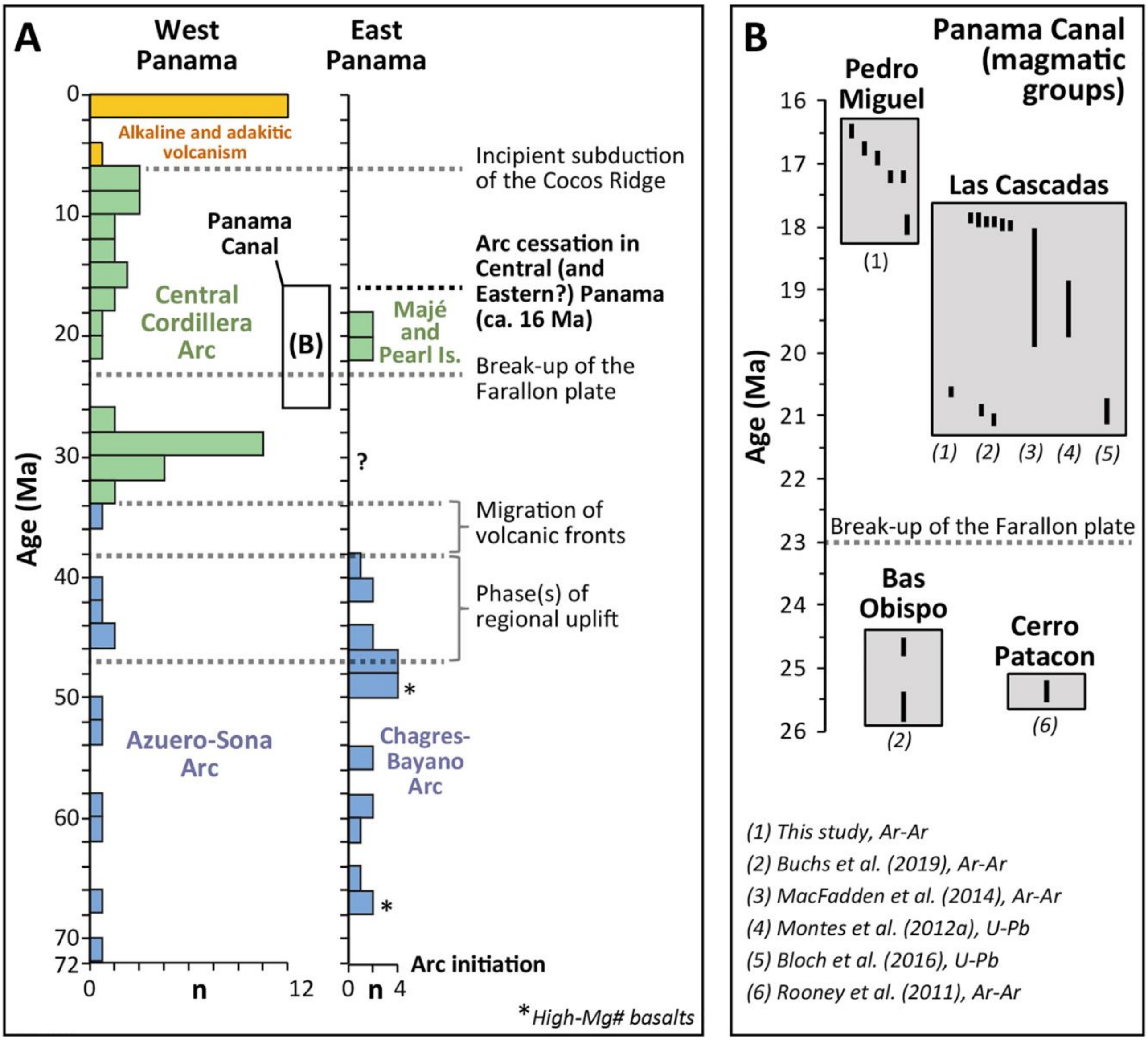

Fig. 2. Synthesis of new and previous geochronological data in Panama and the Canal area, including an interpretation of main regional tectonic events. The source of geochronological data in (A) and (B) is given in the Methods section, with new data of this study (B) shown in Table 1 and Supplementary File 1.

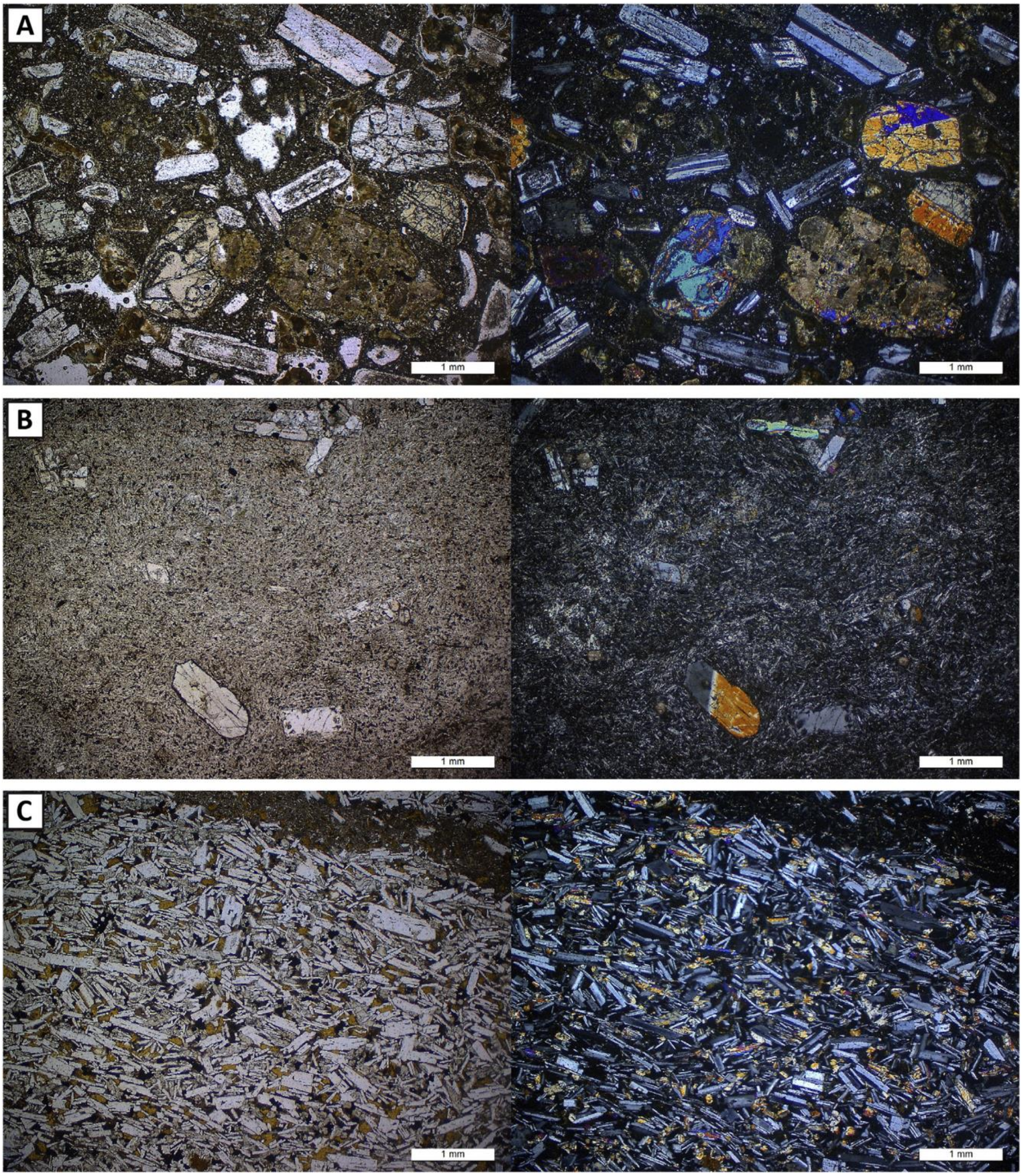

Fig. 3. Typical petrographic characteristics of the main geochemical groups defined along the Gaillard Cut of the Panama Canal (PPL left, XPL right). (A) Clast of basaltic andesite from the Bas Obispo group (sample D16–015), with plagioclase and augite phenocrysts. Matrix and some augites are partly altered to clay. (B) Dacite lava flow from the Las Cascadas group (sample D16–101), with plagioclase and augite phenocrysts. (C) Subvolcanic basaltic andesite from the Pedro Miguel group (sample D16–083). Main phases are plagioclase and augite (light brown in PPL). Glassy interstitial matrix is replaced by clay (orange-brown in PPL). The upper part of the field of view includes a late-stage vein of aphanitic basaltic andesite/andesite. (For interpretation of the references to colour in this figure legend, the reader is referred to the web version of this article.)

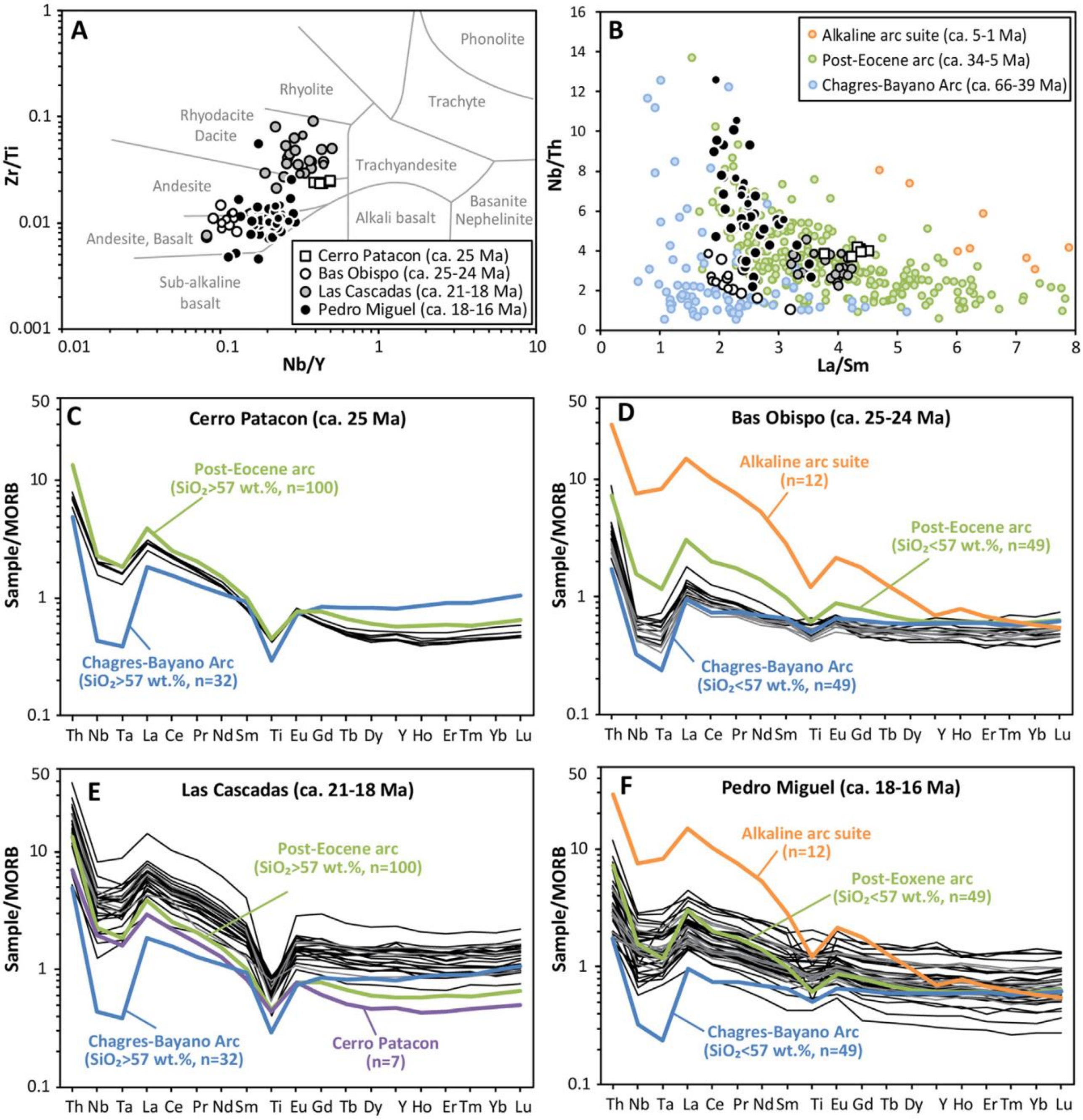

Fig. 4. Selection of trace element diagrams with geochemical groups of the Canal area and regional reference datasets (sources as described in the Methods section). Multi-element diagrams (C-F) are normalised on N-MORB (Gale et al., 2013).

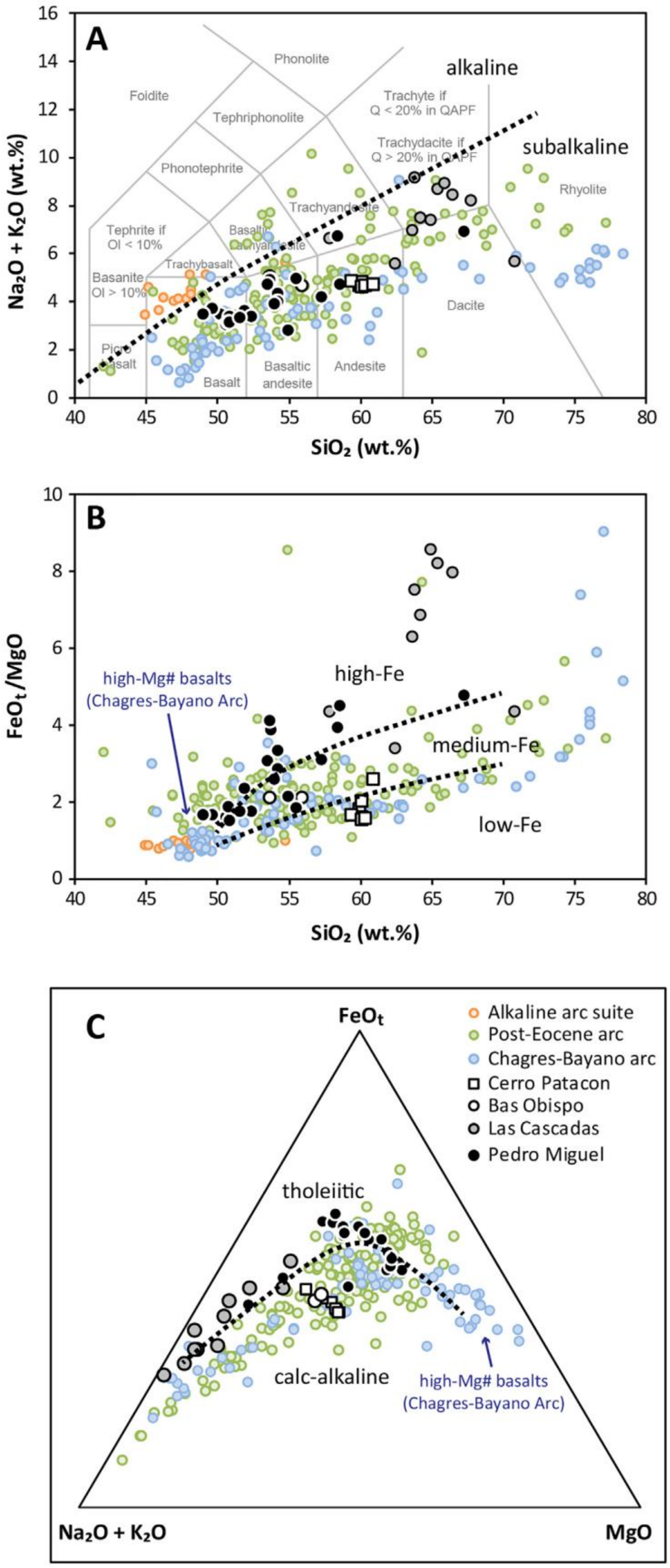

Fig. 5. Selection of major element diagrams with geochemical groups of the Canal area and regional reference datasets (sources as described in the Methods section).

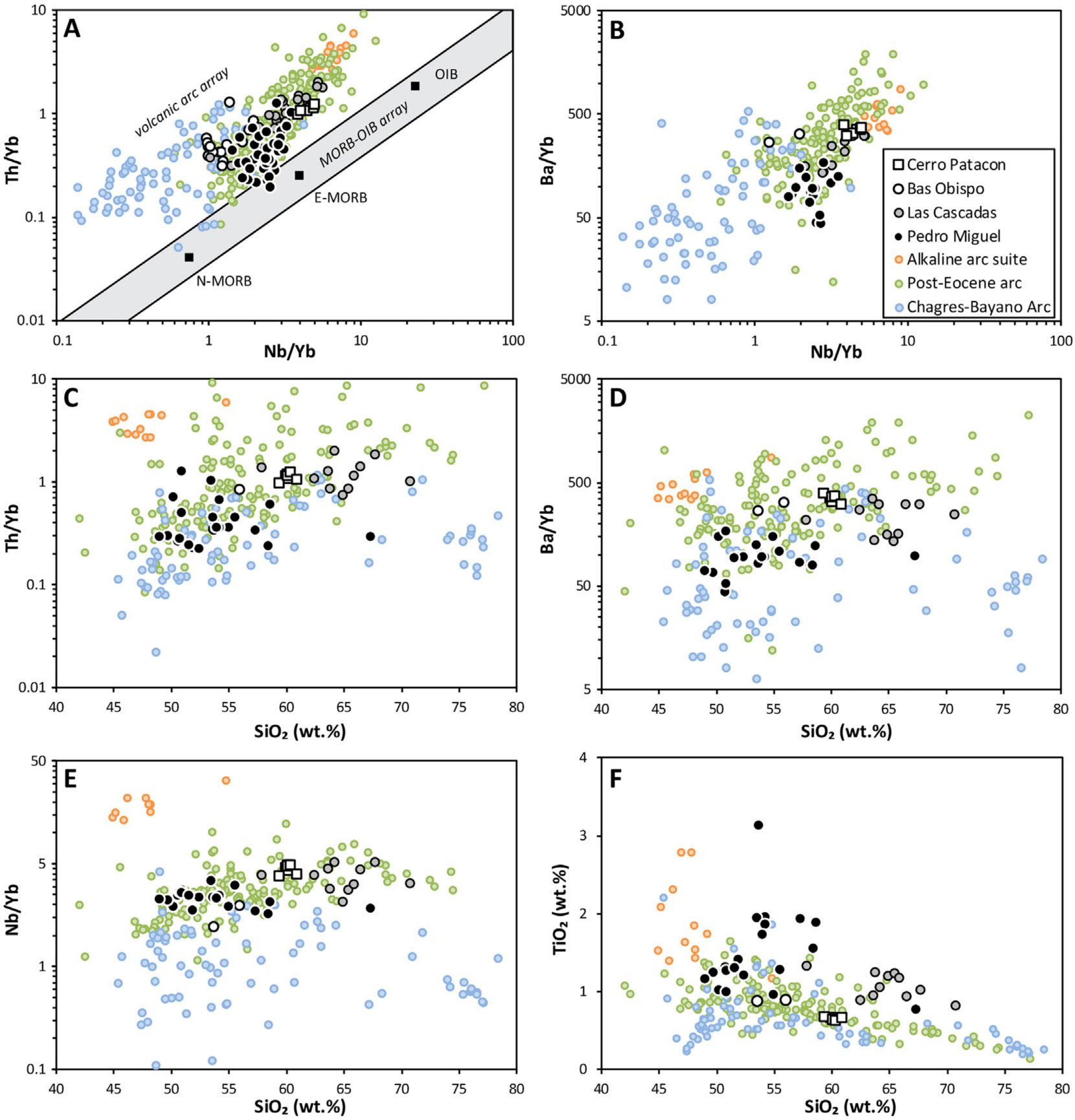

Fig. 6. (A) Nb/Y vs Th/Yb discrimination diagram from Pearce (2008). (B) Nb/Yb vs Ba/Yb diagram. (C–F) SiO2 vs selected trace element ratios and TiO_2. The sources of geochemical groups in the Canal area and regional reference datasets are given in the Methods section.

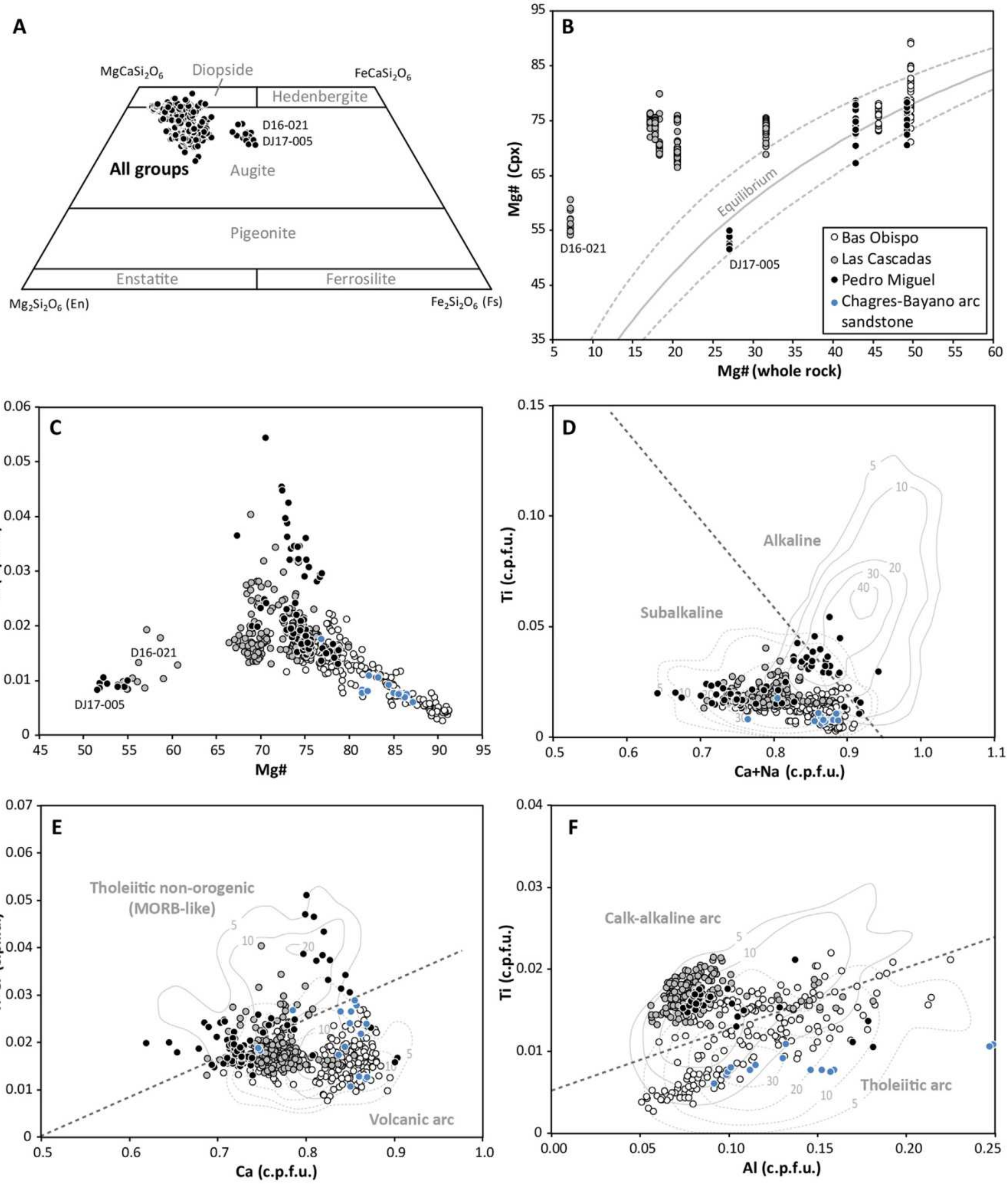

Fig. 7. Pyroxene geochemistry from geochemical groups of the Gaillard Cut (Panama Canal), and a sample of sandstone from the Chagres-Bayano Arc. (A) Classification diagram. (B) Test of equilibrium between the (micro)phenocrysts and their host rock. Equilibrium envelope is based on 2σ error of K_D(Fe-Mg)$^{cpx-liq}$ (see text for detail). (C) Mg# vs Ti (c.p.f.u.=cation per formula unit). (D–F) Discrimination diagrams from Leterrier et al. (1982), including original density envelopes.

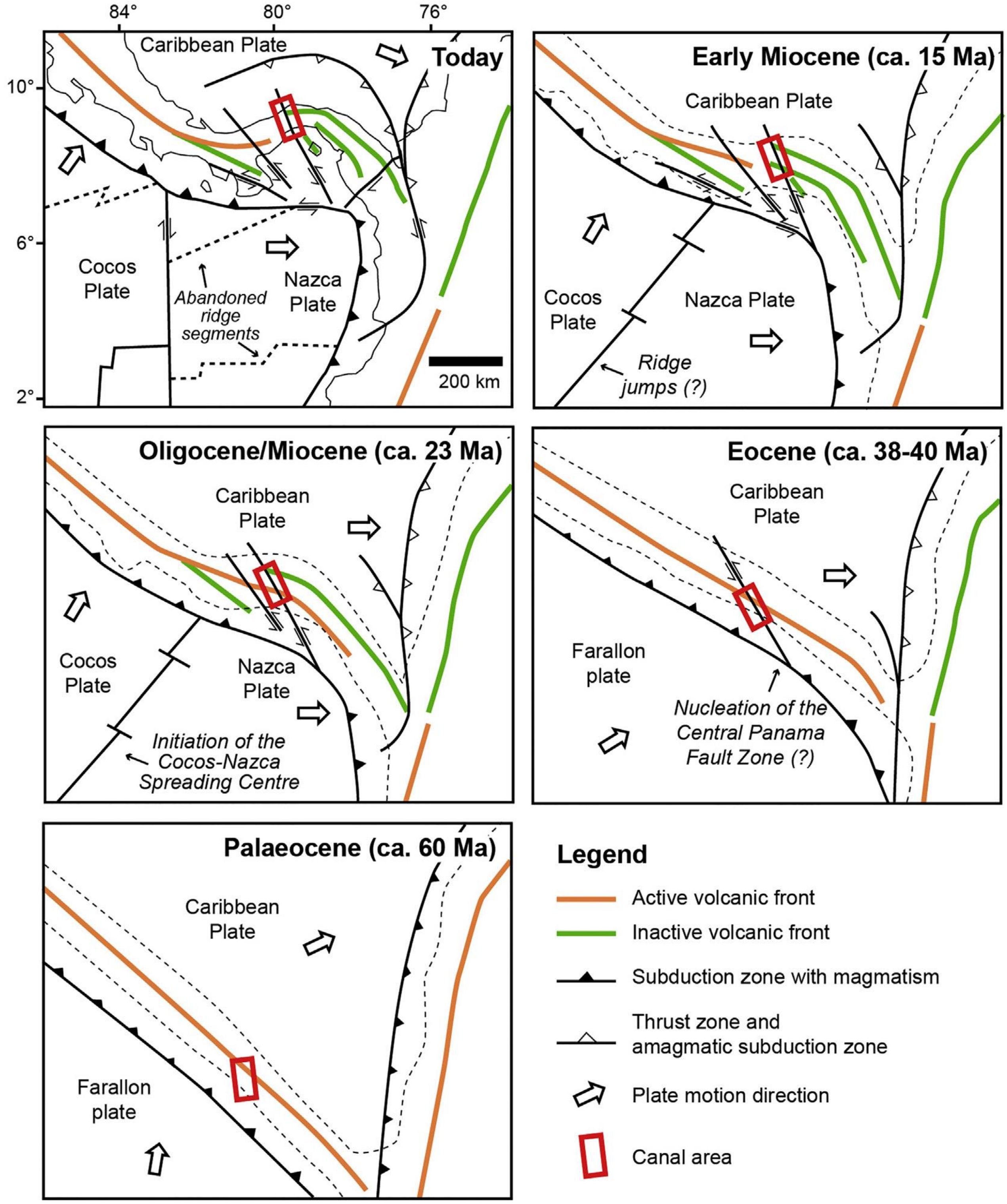

Fig. 8. Tectono-magmatic evolution of the Panama volcanic arc since the Paleocene. The tectonic reconstruction is based on Barat et al. (2014) and is also in agreement with palaeomagnetic and age constraints from Montes et al. (2012b). Abandoned ridge segments on the Cocos and Nazca Plates are based on Meschede et al. (2008). Our model proposes that magmatic cessation in the Canal area (Central Panama) and possibly Eastern Panama ca. 16 Ma resulted from a shift from orthogonal to more oblique subduction along Panama following breakup of the Farallon plate ca. 23 Ma. This model also accounts for the migration of volcanic fronts ca. 40 Ma in Panama, as a possible result of changes in the convergence of the Caribbean and Farallon plates, variation in the Farallon slab angle, and/or initiation of oroclinal bending in Panama due to collision of the Panama volcanic arc with South America.